31st Annual International Conference of the IEEE EMBS
Minneapolis, Minnesota, USA, September 2-6, 2009

Tetrahedral and Polyhedral Mesh Evaluation for Cerebral Hemodynamic Simulation - a Comparison

Martin Spiegel, Thomas Redel, Y. Jonathan Zhang, Tobias Struffert, Joachim Hornegger, Robert G. Grossman, Arnd Doerfler and Christof Karmonik

Abstract— **Computational fluid dynamic (CFD) based on patient-specific medical imaging data has found widespread use for visualizing and quantifying hemodynamics in cerebrovascular disease such as cerebral aneurysms or stenotic vessels. This paper focuses on optimizing mesh parameters for CFD simulation of cerebral aneurysms. Valid blood flow simulations strongly depend on the mesh quality. Meshes with a coarse spatial resolution may lead to an inaccurate flow pattern. Meshes with a large number of elements will result in unnecessarily high computation time which is undesirable should CFD be used for planning in the interventional setting. Most CFD simulations reported for these vascular pathologies have used tetrahedral meshes. We illustrate the use of polyhedral volume elements in comparison to tetrahedral meshing on two different geometries, a sidewall aneurysm of the internal carotid artery and a basilar bifurcation aneurysm. The spatial mesh resolution ranges between 5,119 and 228,118 volume elements. The evaluation of the different meshes was based on the wall shear stress previously identified as a one possible parameter for assessing aneurysm growth. Polyhedral meshes showed better accuracy, lower memory demand, shorter computational speed and faster convergence behavior (on average 369 iterations less).**

I. INTRODUCTION

Advances in hardware and software have enabled the application of CFD in various clinical fields, e.g. cardiology [1] or neuroradiology [2]. Different aspects have been analyzed like patient-specific hemodynamic simulation [3], [4], correlation of wall shear stress (WSS) pattern with the risk of rupture of cerebral aneurysms [5], [6] or hemodynamic characteristics pertaining to the angle of the aneurysm bulb relative to the parent artery [7]. Other CFD studies considered the geometric factors of aneurysms [8], [9], [10], e.g. lesion size or aspect ratio to assess the risk of an aneurysm rupture. In [11], different inflow conditions were investigated to assess its dependence to the WSS distribution in the vicinity of three basilar tip aneurysms. WSS patterns play a major role for assessing pathological vessel systems within the CFD blood flow community.

Most of these simulations utilized tetrahedral meshes. More advanced meshing techniques are now available in turn-key commercial CFD software packages which may lead to a reduction in computing time by reducing the overall number of volume elements while maintaining accuracy. While accurate meshing is essential to obtain mesh-independent results, a deficiency in the mesh may not be obvious and may lead to non-valid results as other incorrect simulation parameters, such as improper inlet conditions in terms of mass or blood flow speed, varying blood density and viscosity, blood modeled as Newtonian fluid. Mesh deficiencies include cells with high skewness factor and a coarse spatial resolution that may lead to imprecision computation of local velocity or WSS pattern. While assessment of the mesh quality is time-consuming, it is nevertheless a very important task. Two distinct approaches for mesh suitability verification have been introduced [12]: 1) Comparison of the numerical simulation results with experimental data and 2) generation of a set of meshes with increasing number of control elements also called mesh independence analysis. Phase-contrast MRI measurements deliver suitable results to compare MR velocity values or primary blood flow patterns with CFD simulation results [13]. Mesh independence analysis is considered the established method for verifying mesh accuracy to simulate arterial flow. It requires a setup of different meshes per vessel geometry from low to high resolution.

The goal of this study was to explore in the framework of mesh independence analysis whether polyhedral meshes with fewer volume elements than comparable tetrahedral meshes will result in better accuracy with shorter computation time using patient-specific imaging data. Two cerebral aneurysm geometries were investigated: one internal carotid and one basilar tip aneurysm, respectively (see Fig. 1). A set of varying mesh resolutions was systematically created as a benchmark for spatial mesh resolutions needed to obtain accurate, mesh-independent WSS patterns or blood flow velocity.

II. METHODS

3-D digital subtraction angiography (DSA) image data [14] of the two cerebral aneurysms (see Fig. 1) were acquired during endovascular interventions using a biplane

M. Spiegel is with Friedrich-Alexander University Erlangen-Nuremberg (FAU), Department of Computer Science, Chair of Pattern Recognition, Germany and FAU, Department of Neuroradiology and Siemens AG Healthcare Sector, Forchheim, Germany and the Erlangen Graduate School in Advanced Optical Technologies (SAOT), Germany martin.spiegel@informatik.uni-erlangen.de

T. Redel is with Siemens AG Healthcare Sector, Forchheim, Germany

J. Zhang is an interventional neuroradiologist and vascular surgeon with The Methodist Hospital, Houston, TX, USA

T. Struffert is an interventional neuroradiologist with FAU, Department of Neuroradiology, Erlangen, Germany

J. Hornegger is with FAU, Department of Computer Science, Chair of Pattern Recognition (Head) and SAOT, Erlangen, Germany

RG Grossman is Chairman of the Department of Neurosurgery and Director of the Neurological Insitute, The Methodist Hospital, Houston, TX USA

A. Doerfler is with FAU, Department of Neuroradiology (Head), Erlangen, Germany

C. Karmonik is a Research Scientist with The Methodist Hospital Research Institute, Houston, TX, USA ckarmonik@tmhs.org

TABLE I

SET OF MESHES - CASE 1 AND CASE 2. TET. AND POLY. ABBREVIATE TETRAHEDRAL AND POLYHEDRAL RESPECTIVELY. PA AND ITER. DENOTE PASCAL AND ITERATIONS.

	#Tet. Cells	Angle	Growth	Max./Min. Triangle	Tet. #Iter.	#Poly. Cells	Poly. #Iter.	Tet. WSS (Pa)	Poly. WSS (Pa)
Case1	13841	25	1.2	6 / 0.001	153	5119	63	9.52	10.33
	26702	14	1.2	3.6 / 0.001	180	7283	81	11.66	11.88
	52374	14	1.1	1.8 / 0.001	296	12467	108	13.37	13.15
	76493	6	1.2	1.2 / 0.001	306	17695	122	14.53	13.80
	86621	12	1.1	0.4 / 0.001	1633	18681	142	14.43	13.92
	106010	12	1.1	0.36 / 0.001	1291	22297	185	14.76	13.99
	115014	10	1.1	0.3 / 0.001	451	25540	154	14.71	14.32
	228118	10	1.1	0.25 / 0.001	-	43487	583	-	15.58
Case2	31696	17	1.2	0.42 / 0.001	242	8814	111	5.91	5.26
	43063	17	1.17	0.37 / 0.001	378	10843	176	7.18	6.20
	56176	15	1.12	0.34 / 0.001	365	13280	185	7.06	6.51
	75469	13	1.10	0.32 / 0.001	437	16795	202	7.33	6.84
	98399	10	1.10	0.3 / 0.001	462	21108	211	7.43	7.15
	114227	10	1.10	0.28 / 0.001	496	23846	230	7.47	7.23
	148625	8	1.09	0.25 / 0.001	714	30167	269	7.62	7.45
	174225	6	1.10	0.24 / 0.001	626	35665	254	7.48	7.57

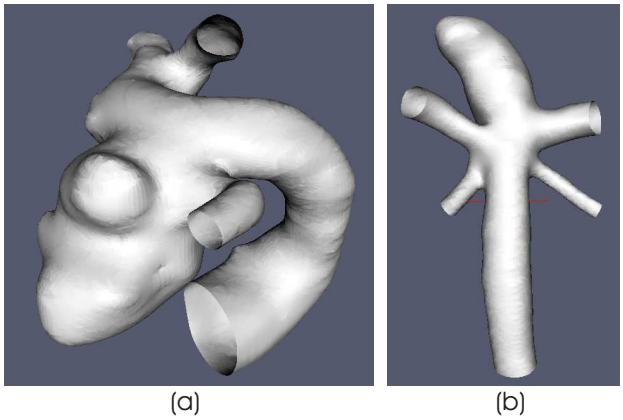

Fig. 1. Three dimensional reconstruction of the evaluated aneurysms: (a) Case1 depicts a internal carotid aneurysm (b) Case2 illustrates a basilar tip aneurysm

flat-panel system Siemens C-Arm System (dBA, Siemens AG Healthcare Sector) in Erlangen (Germany) and Houston (USA). 3-D image reconstructions of both aneurysms led to an image volume for Case1 of 138.24×138.24×57.72mm with a voxel spacing of 0.27×0.27×0.13mm and for Case2 97.28×97.26×66.43mm (voxel spacing 0.19×0.19×0.1mm) respectively. For mesh generation and smoothing, the Marching Cubes [15] and a Laplacian-based smoothing algorithm (VTK Kitware Inc.) was applied as an addtional step. The image data was stored as a stereolithographic file (STL) providing the input data for the commercial meshing software GAMBIT (ANSYS Inc.).

The GAMBIT curvature size function [16] was used to easily generate different surface meshes exhibiting a granularity from coarse to fine. This function constrains the angle between outward-pointing normals for any two adjacent surface triangles. That is particularly useful in the case of highly curved surfaces like aneurysm geometries. Hence, regions with high curvature are meshed in more detail than those with lower curvature. Four parameters define the curvature size function i.e. angle in degree, growth in percentage, max. and min. triangle size. Table I contains a detailed overview of the applied curvature size function parameters. Given a certain geometry and certain parameter values, the meshing algorithm will automatically choose the final number of triangles for the surface mesh.

The number of tetrahedral mesh elements for the whole volume depends on the resolution of the given surface mesh - the larger the number of triangles, representing the surface, the larger the number of tetrahedral mesh elements.

Meshes were imported into the simulation software Fluent (ANSYS Inc.). For each tetrahedral mesh a corresponding polyhedral mesh was generated by a conversion algorithm part of the Fluent CFD solver. The surface of the aneurysm and the parent artery were modeled as rigid-walls and no slip as shear condition. Blood was modeled as an incompressible Newtonian fluid with a density of 1050kg/m^3 and a viscosity of 0.004 N/m^{2}s [17]. The boundary conditions for all conducted simulations were as follows: the inlet was considered as a velocity inlet and all outlets were modeled as pressure outlet zero. A constant inflow rate of 0.5 m/s was applied in the steady simulations. We considered a steady-state simulation as converged, if the relative residuals falls under 0.001 (i.e. the absolute values of the residuals were reduced by three orders of magnitude). A series of steady-state simulations were performed according to the meshes shown in table I in order to eliminate the issue of unsuitable CFD meshes and to compare the results given from polyhedral and tetrahedral meshes. Figure 2 gives an overview about the simulation results concerning WSS distribution. The Area-Weighted-Average WSS distribution was used to analyze the WSS differences between polyhedral and tetrahedral meshes in terms of numbers. It is defined as

$$\frac{1}{A}\int \phi dA = \frac{1}{A}\sum_{i=1}^{n} \phi_i \left|A_i\right| \tag{1}$$

where A denotes the total area being considered and ϕ_i describes the wall shear stress associated with the facet area A_i.

III. RESULTS

The simulation series shows two findings. 1) the WSS pattern of polyhedral meshes look more homogeneous than the ones of the tetrahedral meshes as indicated by the yellow circles in figure 2. Table I (columns 9 and 10) depicts the values of the average Area-Weighted-Average WSS distribution considering only the aneurysm area as illustrated in figure 2. The differences between both mesh types are negligible considering the fact that polyhedral meshes exhibit far less cell elements than tetrahedral meshes. 2) tetrahedral meshes exhibit a far worse convergence as the polyhedral ones (see table I column 6 and 8). On average, tetrahedral meshes need 369 iterations more than the polyhedral meshes. The highest resolved tetrahedral mesh (case1 228118 tetrahedral elements) did not converge according to the applied boundary condition as described in the method section.

IV. DISCUSSION

A certain mesh resolution is needed to resolve the WSS distribution on a valid base. The WSS pattern is similar for tetrahedral (when converged) and polyhedral. However, it changes with increasing spatial resolution and converges at a certain level (see figure 2 and table I). Polyhedral meshes can be considered as a viable alternative to tetrahedral meshes because they do not only show better computational convergence [18]. They are also able to resolve the WSS pattern with far less control volumes per mesh in a more homogeneous manner than the tetrahedral meshes. The reason for this lies in the way the WSS magnitude is calculated which depends on two major aspects: 1) only those cell elements are considered which actually share a face with the vessel boundary. Not all tetrahedral elements located at the vessel boundary share necessarily an entire face with the boundary - some may touch the boundary with its corner. While all polyhedral elements located at the wall share an entire face with the boundary itself. 2) The distances of the considered tetrahedral centers are not equal to the vessel wall leading to a more inhomogeneous WSS appearance.

From a clinical perspective, the convergence as well as the computation speed of CFD simulations are crucial aspects regarding future clinical CFD-based diagnostic and treatment tools. It is not feasible for the treating physician to have to change simulation parameters to optimize convergence behavior. Our evaluation has shown that the polyhedral-based meshes are more stable and faster and should be used in a future standardized clinical simulation workflow.

The results obtained during this study may be affected due to several limitations. Our assumptions concerning the conducted CFD experiments differ from the *in vivo* state in terms of rigid vessel walls, Newtonian-based blood fluid and the determination of the boundary conditions, respectively. The outflows of the patient-specific models are defined as pressure outlet zero which does not have to match with the real environment. There might be natural resistances at the outflows. As with other computational studies, it is assumed that these limitations have only minor effects on the resulting flow pattern [19]. However, future work has to focus on the reduction of these limitation in the sense of validation against *in vivo* measurements.

V. CONCLUSION

This study represents the first mesh independency analysis in the field of cerebral blood flow simulation together with a comparison of polyhedral and tetrahedral-based meshes. Here, we put the focus from the actual flow pattern within aneurysms or its corresponding WSS pattern to the evaluation of the CFD mesh. Our results illustrate the importance of a well-founded mesh granularity evaluation before starting a blood flow simulation in order to get reliable blood flow simulation results to support the clinical decision making. This approach serves as a first key step towards a future clinical CFD application where the mesh generation process has to be automated as much as possible. Furthermore, the results will allow to deviate requirements to geometric model accuracy acquired by modern imaging methods and to optimize CFD computation time without loss of accuracy.

VI. ACKNOWLEDGMENTS

The authors would like to thank Dr. Ralf Kroeger (ANSYS Germany GmbH) for his advice and simulation support. The authors gratefully acknowledge funding of the Erlangen Graduate School in Advanced Optical Technologies (SAOT) by the German National Science Foundation (DFG) in the framework of the excellence initiative.

REFERENCES

[1] A. Theodorakakos, M. Gavaises, A. Andriotis, A. Zifan, P. Liatsis, I. Pantos, E. Efstathopoulos, and D. Katritsis, "Simulation of cardiac motion on non-newtonian, pulsating flow development in the human left anterior descending coronary artery," *Physics in Medicine and Biology*, vol. 53, pp. 4875–4892, 2008.

[2] C. Karmonik, A. Arat, G. Benndorf, S. Akpek, R. Klucznik, M. Mawad, and C. Strother, "A technique for improved quantitative characterization of intracranial aneurysms," *American Journal of Neuroradiology*, vol. 25, no. August, pp. 1158–1161, 2004.

[3] D. Steinman, J. Milner, C. Norley, S. Lownie, and D. Holdsworth, "Image-based computational simulation of flow dynamics in a giant intracraniel aneurysm," *American Journal of Neurradiology*, vol. 24, pp. 559–566, April 2003.

[4] M. Castro, C. Putman, and J. Cebral, "Patient-specific computational fluid dynamics modeling of anterior communicating artery aneurysms a study of the sensitivity of intra-aneurysmal flow patterns to flow conditions in the carotid arteries." *American Journal of Neurradiology*, vol. 27, pp. 2061–2068, 2006.

[5] L. Jou, D. Lee, H. Morsi, and M. Mawad, "Wall shear stress on ruptured and unruptured intracranial aneurysms at the internal carotid artery," *American Journal of Neurradiology*, vol. 29, pp. 1761–1767, October 2008.

[6] J. Cebral, M. Castro, J. Burgess, R. Pergolizzi, M. Sheridan, and C. Putman, "Characterization of cerebral aneurysms for assessing risk of rupture by using patient-specific computational hemodynamics models." *American Journal of Neurradiology*, vol. 26, pp. 2550–2559, 2005.

[7] M. Ford, S. Lee, S. Lownie, D. Holdsworth, and D. Steinman, "On the effect of parent-aneurysm angle on flow patterns in basilar tip aneurysms: Towards a surrogate geometric marker of intra-aneurismal hemodynamics," *Journal of Biomechanics*, vol. 41, pp. 241–248, 2008.

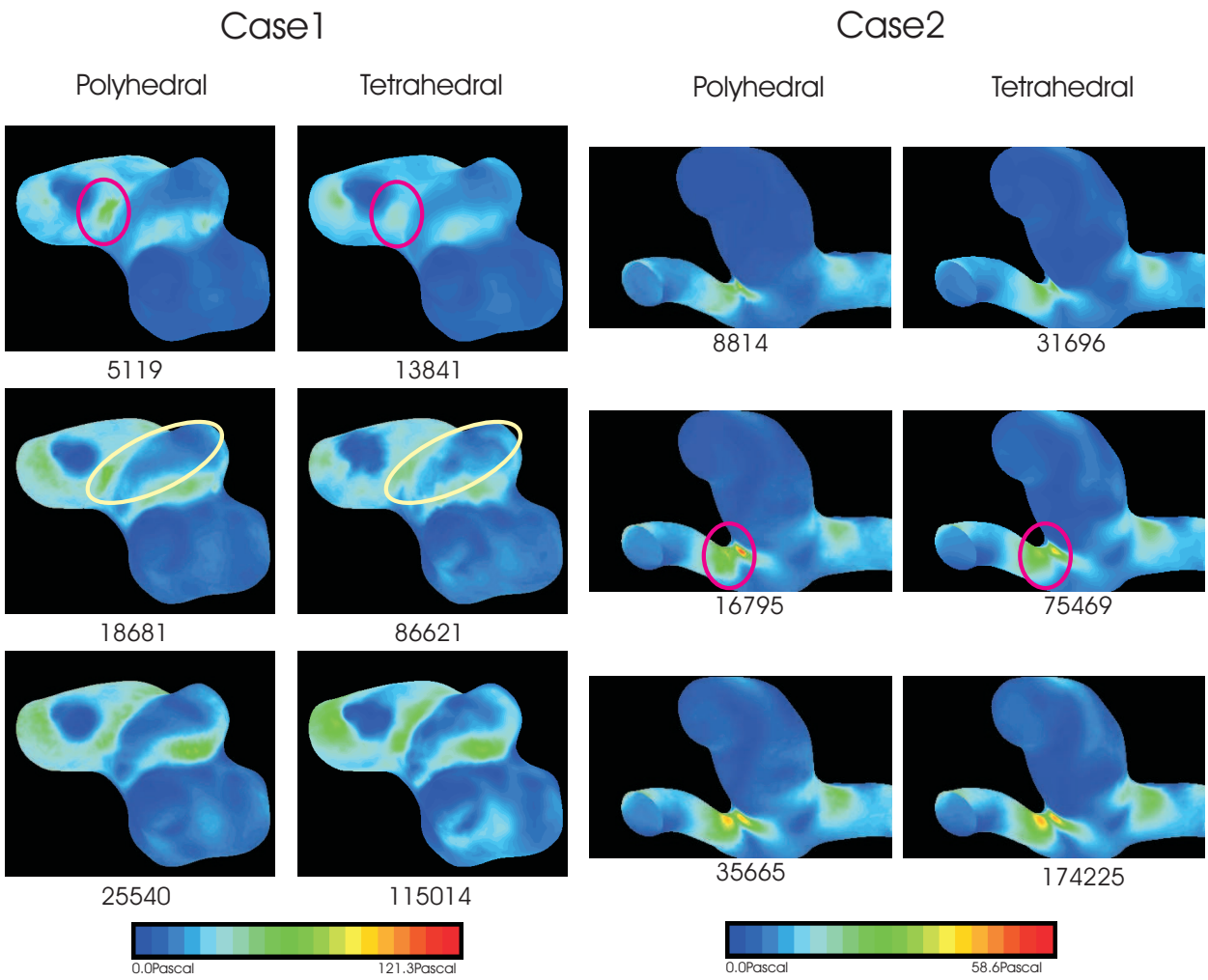

Fig. 2. WSS distribution for polyhedral and tetrahedral meshes. The WSS patterns computed from polyhedral meshes appear more homogeneous than tetrahedral-based WSS patterns (see yellow circles). Polyhedral meshes were also able to represent significant WSS pattern with fewer cells than tetrahedral ones as marked by the red circles. The numbers below the individual figures denote the number of cells of the mesh.

[8] H. Ujiie, Y. Tamano, K. Sasaki, and T. Hori, "Is the aspect ratio a reliable index for predicting the rupture of a saccular aneurysm?" *Neurosurgery*, vol. 48, p. 495502, 2001.

[9] A. Nader-Sepahi, M. Casimiro, J. Sen, and N. Kitchen, "Is aspect ratio a reliable predictor of intracranial aneurysm rupture?" *Neurosurgery*, vol. 54, p. 13431347, 2004.

[10] M. Raghavan, B. Ma, and R. Harbaugh, "Quantified aneurysm shape and rupture risk," *Journal of Neurosurgery*, vol. 102, p. 355362, 2005.

[11] C. Karmonik, G. Benndorf, R. Klucznik, H. Haykal, and C. Strother, "Wall shear stress variations in basilar tip aneurysms investigated with computational fluid dynamics," in *Engineering in Medicine and Biology*, 2006.

[12] S. Prakash and C. R. Ethier, "Requirements for mesh resolution in 3d computational hemodynamics," *Journal of Biomechanical Engineering*, vol. 123, pp. 134–144, April 2001.

[13] C. Karmonik, R. Klucznik, and G. Benndorf, "Blood flow in cerebral aneurysms: comparison of phase contrast magnetic resonance and computational fluid dynamics–preliminary experience," vol. 180, no. 3, pp. 209–215, 2008.

[14] N. Heran, J. Song, K. Namba, W. Smith, Y. Niimi, and A. Berenstein, "The utility of dynact in neuroendovascular procedures," *American Journal of Neurradiology*, vol. 27, pp. 330–332, February 2006.

[15] H. Lorensen, W. E. Cline, "Marching cubes: A high resolution 3d surface construction algorithm," *Computer Graphics*, vol. 21, no. 4, pp. 163–169, 1987.

[16] F. Cooperation, *Gambit 2.4 User's Guide*. E.I. du Pont de Nemours and Co., 2007.

[17] T. Hassan, M. Ezura, E. Timofeev, T. Tominaga, T. Saito, A. Takahashi, K. Takayama, and T. Yoshimoto, "Computational simulation of therapeutic parent artery occlusion to treat giant vertebrobasilar aneurysm," *American Journal of Neurradiology*, vol. 25, pp. 63–68, January 2004.

[18] M. Peric, "Flow simulation using control volumes of arbitrary polyhedral shape," in *ERCOFTAC Bulletin*, no. 62, September 2004.

[19] J. Cebral, M. Castro, S. Appanaboyina, C. Putman, D. Millan, and A. Frangi, "Efficient pipeline for image-based patient-specific analysis of cerebral aneurysm hemodynamics: technique and sensitivity," *IEEE Transactions on Medical Imaging*, vol. 24, pp. 457–467, 2005.